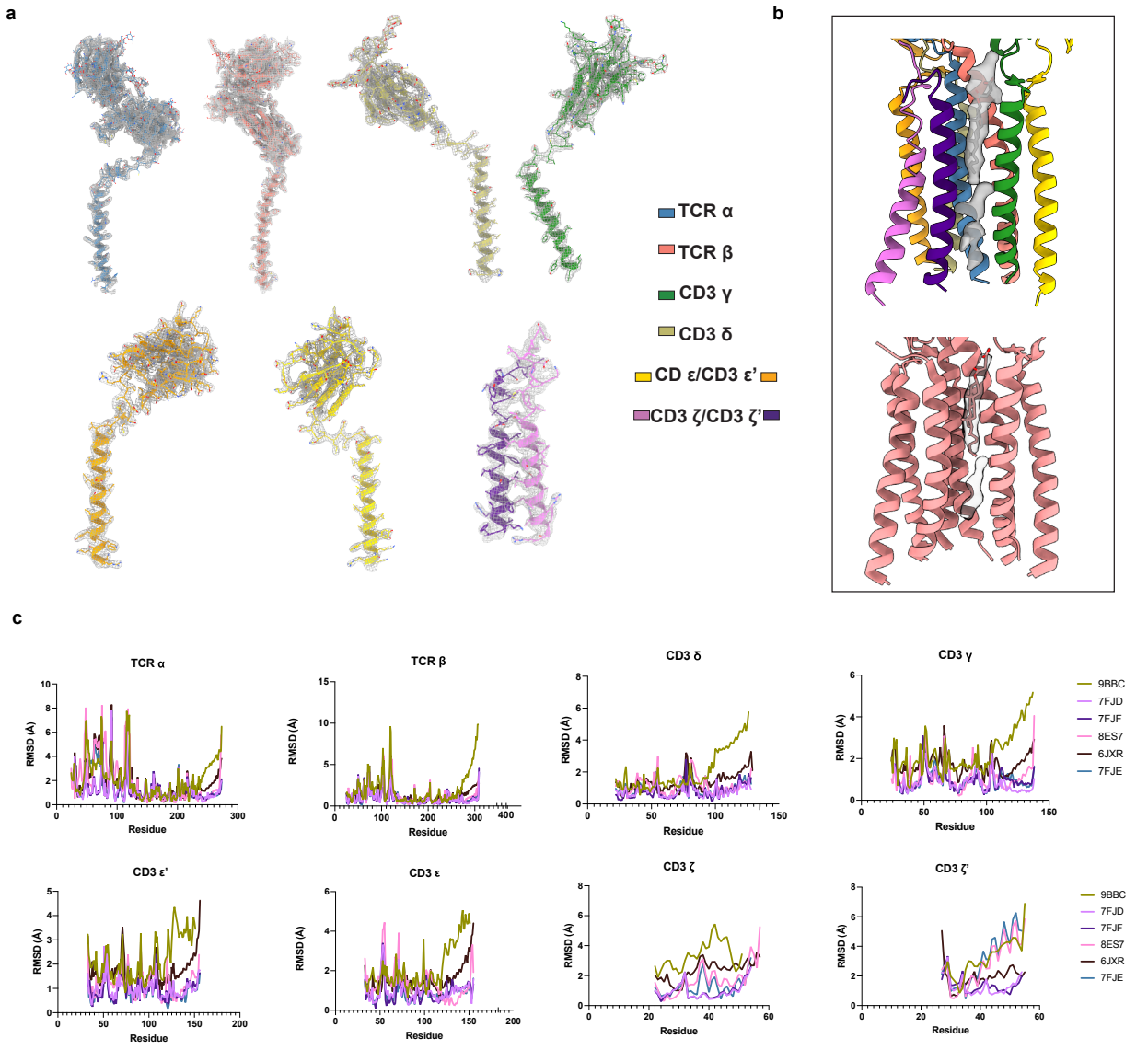

Supplementary Figure 1. Apo-TCR$^{M1(58-66)}$/CD3 structural analysis. a. Model of each chain fit into density map showing clear side chains. Density maps are shown as mesh. **b**. Density observed in CLR1 and tentative CLR2 binding sites this study and in PDB 8ES7. Top panel shows the two lipid densities observed in these sites in this study. Upper density supports previously claimed cholesterol occupation in the CLR1 binding site, but lower density in the tentative CLR2 site does not cooperate cholesterol occupancy of this site. We modeled a cholesterol molecule in the upper density. Bottom panel shows two lipid densities observed in the CLR1 and CLR2 sites in EMD-28570/PDB 8ES7. Upper density supports previously claimed cholesterol occupancy in the CLR1 binding site, but lower density does not cooperate cholesterol

occupancy in the CLR2 site. **c**. Single amino acid RMSD scanning of each chain of apo-TCR$^{M1(58\text{-}66)}$/CD3 with multiple published TCR/CD3 complexes. All models were superimposed with apo-TCR$^{M1(58\text{-}66)}$/CD3 and alpha carbon, nitrogen, carbon and oxygen backbone atom distances of each chain residue were calculated.

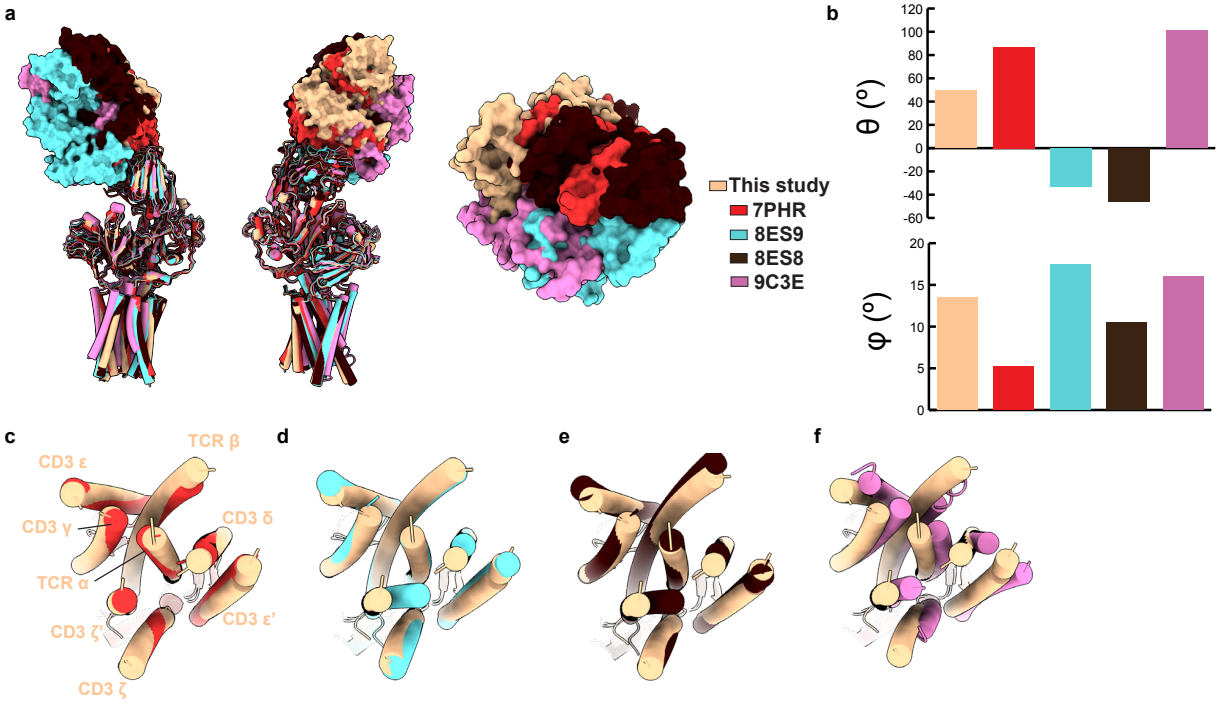

Supplementary Figure 2. Structural comparison of pHLA-A*02:01$^{M1(58-66)}$/TCR$^{M1(58-66)}$/CD3 complex with published pMHCI/TCR/CD3 complexes. a. Superimposition of pHLA-A*02:01$^{M1(58-66)}$/TCR$^{M1(58-66)}$/CD3 with multiple published pMHCI/TCR/CD3 complexes. pMHCI components are displayed as surface and TCR/CD3 components are displayed as cartoon. **b.** Binding angle analysis of our pHLA-A*02:01$^{M1(58-66)}$/TCR$^{M1(58-66)}$/CD3 compared to other pMHCI/TCR/CD3 complexes. **c-f.** pHLA-A*02:01$^{M1(58-66)}$/TCR$^{M1(58-66)}$/CD3 transmembrane helix positions compared to other pMHCI/TCR/CD3 complexes viewed from the cytoplasmic side.

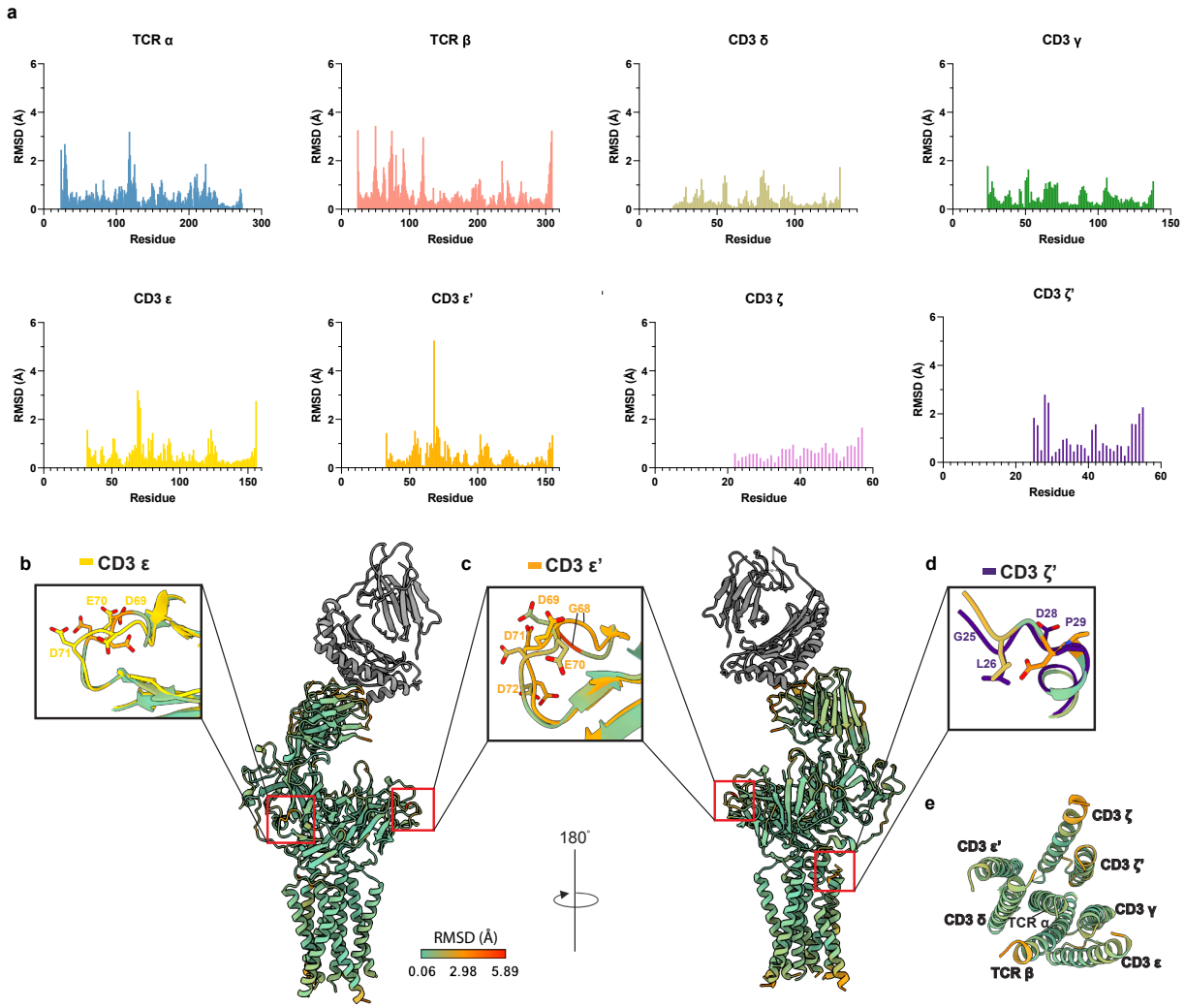

Supplementary Figure 3. Structural comparison of apo-TCR$^{M1(58-66)}$/CD3 and pHLA-A*02:01$^{M1(58-66)}$/TCR$^{M1(58-66)}$/CD3. a. Cα RMSD of each chain residue was calculated and plotted. **b-e.** pHLA-A*02:01$^{M1(58-66)}$/TCR$^{M1(58-66)}$/CD3 shows detailed chain movement of CD3 ε, ε', ζ'. **b.** CD3 ε chain peripheral loop movement between apo-TCR$^{M1(58-66)}$/CD3 and pHLA-A*02:01$^{M1(58-66)}$/TCR$^{M1(58-66)}$/CD3. TCR$^{M1(58-66)}$/CD3 parts are colored as RMSD distribution. pHLA-A*02:01$^{M1(58-66)}$ is colored in grey. **c.** CD3 ε' chain peripheral loop movement. **d.** Extracellular domain movement of CD3 ζ' chain. **e.** Movements of intracellular side of each TCR/CD3 chain.

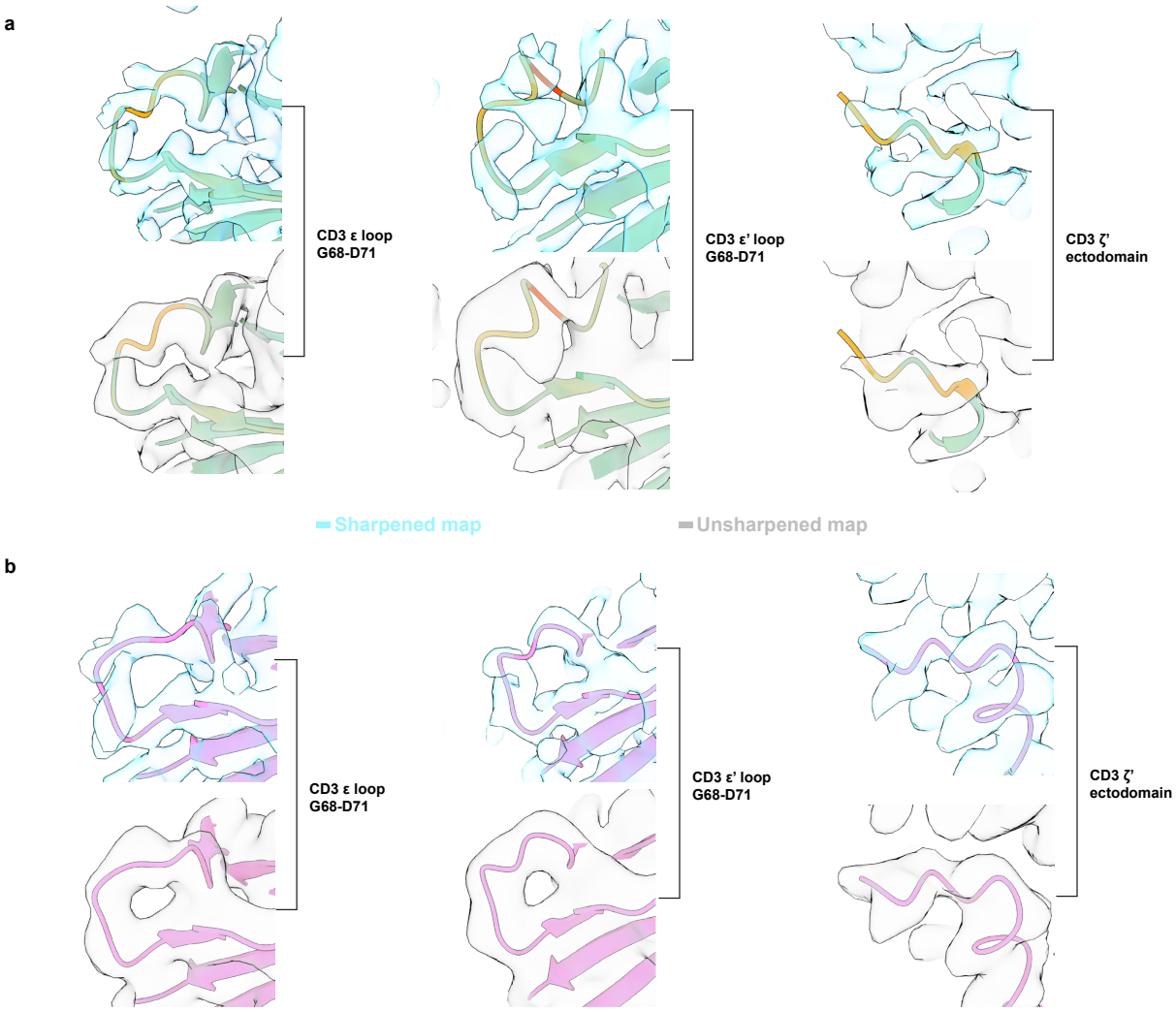

Supplementary Figure 4. The placement of CD3 ε, ε' and ζ' loops. a. pHLA-A*02:01$^{M1(58-66)}$/TCR$^{M1(58-66)}$/CD3 and corresponding density map. **b.** Apo-TCR$^{M1(58-66)}$/CD3 and corresponding density map. Top panels show the fit to sharpened map and bottom panels show the fit to unsharpened map. Sharpened and unsharpened maps are displayed as transparent.

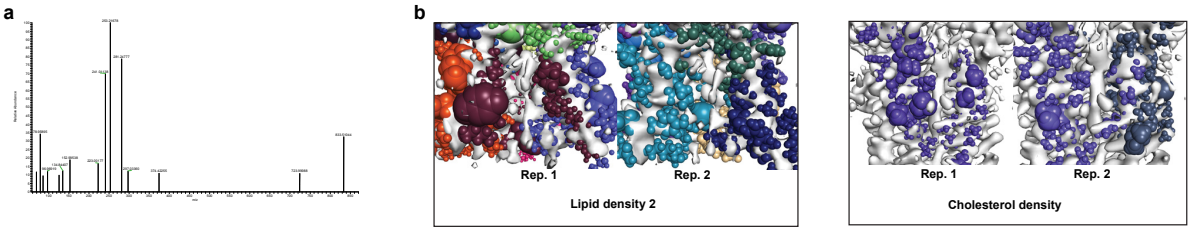

Supplementary Figure 5. **Supplemental data of Lipidomics and LipIDens analysis. a.** Raw plot of detected PI lipid in lipidomics data. **b.** Binding sites identified for Lipid density 2 (left panel) and cholesterol density in CLR1 binding site (right panel) in two replicates of LipIDens analysis.

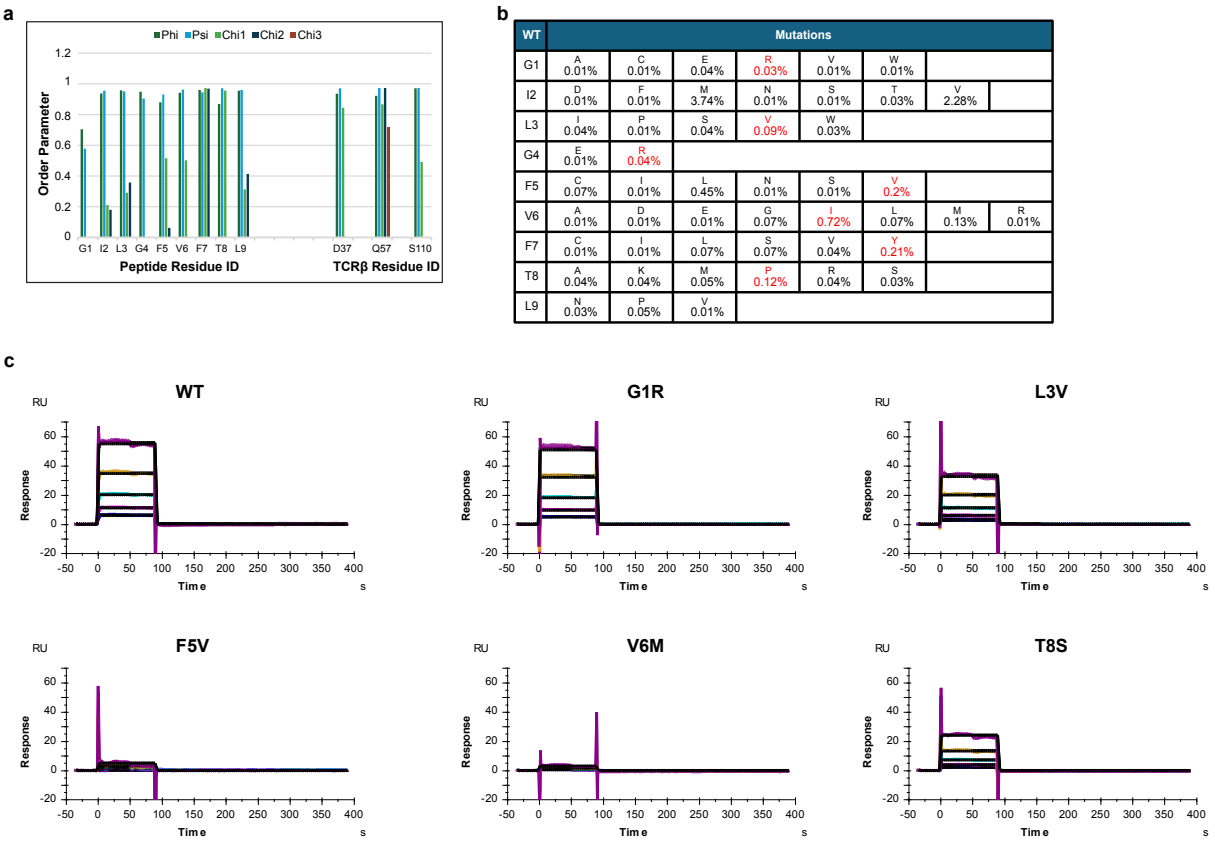

Supplementary Figure 6. MD simulation and SPR analysis of TCR$^{M1(58-66)}$ contacting pHLA-A*02:01. a. Order parameters for ϕ,ψ,Ω, and χ angles for the M1(58-66) peptide and for select TCR residues forming hydrogen bonds with the pMHC complex. **b.** Occurrence of circulating Influenza A M1(58-66) peptide mutants by percentage. Mutant percentage was calculated from the Influenza Resource Database from National Center for Biotechnology Information (NCBI). **c.** SPR raw reading responses related to Figure 7.

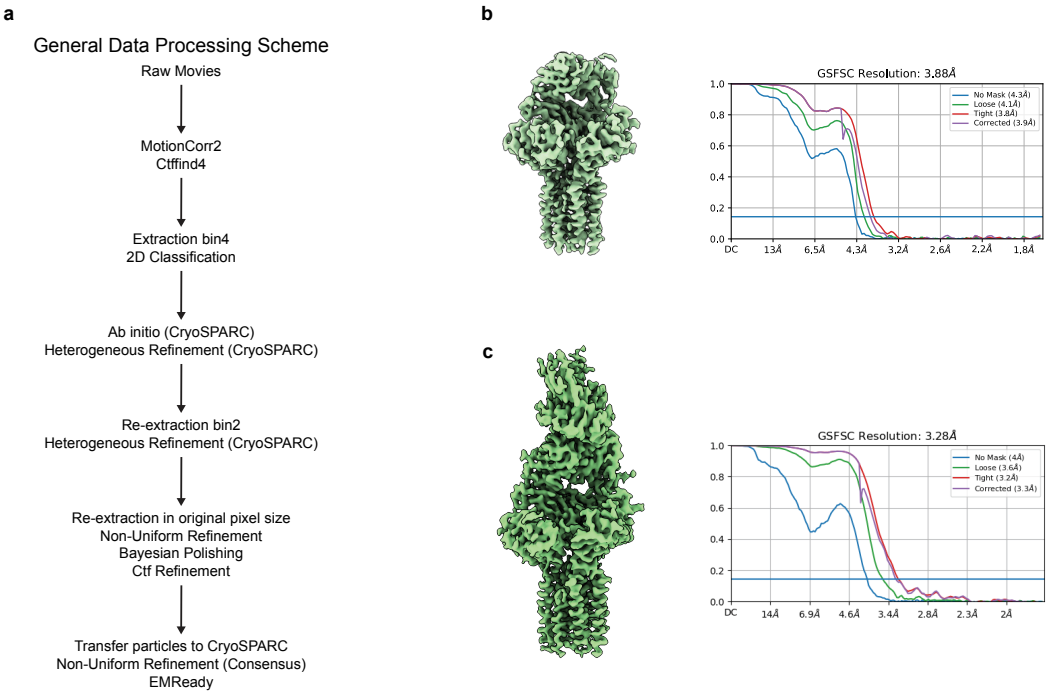

Supplementary Figure 7. **Cryo-EM data processing of apo TCR$^{M1(58-66)}$/CD3 and pHLA-A*02:01$^{M1(58-66)}$/TCR$^{M1(58-66)}$/CD3. a.** General data processing scheme. **b.** Apo TCR$^{M1(58-66)}$/CD3. **c.** pHLA-A*02:01$^{M1(58-66)}$ density map and corresponding GSFSC curve plots.